Atmos. Meas. Tech. Discuss., 7, 12323–12355, 2014
www.atmos-meas-tech-discuss.net/7/12323/2014/
doi:10.5194/amtd-7-12323-2014

Atmospheric Measurement Techniques Discussions

Application of GC/Time-of-Flight-MS for halocarbon trace gas analysis and comparison with GC/Quadrupole-MS

J. Hoker, F. Obersteiner, H. Bönisch, and A. Engel

Institute for Atmospheric and Environmental Science, Goethe University Frankfurt, Frankfurt, Germany

Received: 5 November 2014 – Accepted: 26 November 2014 – Published: 10 December 2014

Correspondence to: A. Engel (an.engel@iau.uni-frankfurt.de)

Published by Copernicus Publications on behalf of the European Geosciences Union.

Abstract

We present the application of Time-of-Flight Mass Spectrometry (TOF MS) for the analysis of halocarbons in the atmosphere, after cryogenic sample preconcentration and gas chromatographic separation. For the described field of application, the Quadrupole Mass Spectrometer (QP MS) is the state-of-the-art detector. This work aims at comparing two commercially available instruments, a QP MS and a TOF MS with respect to mass resolution, mass accuracy, sensitivity, measurement precision and detector linearity. Both mass spectrometers are operated on the same gas chromatographic system by splitting the column effluent to both detectors. The QP MS had to be operated in optimised Single Ion Monitoring (SIM) mode to achieve a sensitivity which could compete with the TOF MS. The TOF MS provided full mass range information in any acquired mass spectrum without losing sensitivity. Whilst the QP MS showed the performance already achieved in earlier tests, the sensitivity of the TOF MS was on average higher than that of the QP MS in the "operational" SIM mode by a factor of up to 3 reaching detection limits of less than 0.2 pg. Measurement precision determined for the whole analytical system was up to 0.2 % depending on substance and sampled volume. The TOF MS instrument used for this study displayed significant non-linearities of up to 10 % for two third of all analysed substances.

1 Introduction

With increasing evidence that anthropogenic chlorinated and brominated hydrocarbons can be transported into the stratosphere and release chlorine and bromine atoms there which can deplete ozone in catalytic cycles (Molina and Rowland, 1974; Farman et al., 1985; Solomon, 1990), the production and use of such species was regulated under the Montreal Protocol in 1987. Most of this fully halogenated compounds are declining in the atmosphere (Montzka and Reimann, 2011). However, many partially halogenated compounds are still increasing in the atmosphere (Montzka and Reimann, 2011), as

AMTD
7, 12323–12355, 2014

are some newly detected fully halogenated species (Laube et al., 2014). Also, many fluorocarbons which do not destroy stratospheric ozone and are thus not regulated under the Protocol show increasing trends in the atmosphere (Laube et al., 2012; Ivy et al., 2012; Vollmer et al., 2011). Although these fluorocarbons do not destroy ozone, many of them are strong greenhouse gases with long atmospheric lifetimes, resulting in increased radiative forcing of the troposphere. Therefore, the need persists for continuous measurements to identify new compounds in the atmosphere and monitor and document their atmospheric trends. The mass spectrometric instrument type commonly used for halocarbon analysis is the quadrupole mass spectrometer (QP MS) (Cooke et al., 2001; Miller et al., 2008; Sala et al., 2014). Besides the QP MS, the use of high mass resolving and extremely sensitive sector field MS has also been reported (Lee et al., 1995; Laube et al., 2014). Both sector field and QP MS generally only measure one mass or a few selected masses at a time despite having scanning capabilities. Nevertheless, TOF MS has only been applied sporadically for measurements of atmospheric trace gases (Kim and Kim, 2012; Kundel et al., 2012; Jordan et al., 2009) and in particular not for halocarbons. The main advantage of coupling a TOF MS to a gas chromatograph (GC) over using the QP MS is the intrinsic full mass range acquisition which constitutes, desirably in combination with a high mass resolution and mass accuracy, an advantage for unambiguous substance identification. In contrast, a QP MS is a mass filter and will only measure one mass at a time. It needs to scan many individual masses sequentially to register a full mass spectrum. To achieve high sensitivity, QP MS are therefore often operated in single ion monitoring (SIM) mode where the instrument is tuned to only one or a few selected ion masses and all other ions do not pass the quadrupole mass filter. Regardless of these limitations of the QP MS, it is widely used in analytical chemistry due to its stability, ease of operation, high degree of linearity, good reproducibility as well as sensitivity.

In this paper, a comparison of a state-of-the-art QP MS and a TOF MS is presented, with both mass spectrometers being coupled to the same gas chromatographic system. The instrumental setup is described in Sect. 2. The GC QP MS system was charac-

AMTD
7, 12323–12355, 2014

terised and used before for studies by (Laube and Engel, 2008; Brinckmann et al., 2012) and showed consistent results in the international comparison IHALACE (International Halocarbons in Air Comparison Experiment) with the NOAA (National Oceanic and Atmospheric Administration) network (Hall et al., 2013). We discuss the use of TOF MS in atmospheric trace gas measurements, in particular for the detection and quantification of halocarbons, focusing on four substances: CFC-11, CFC-12, Halon-1211 and Iodomethane. These four substances cover the boiling point and typical concentration range of a total of 35 substances analysed. The five key parameters for atmospheric trace gas measurements discussed in this paper are (1) mass resolution and (2) mass accuracy of the detectors, (3) detector sensitivity represented by the limits of detection (LOD), (4) reproducibility of the measurement procedure and (5) the linearity of the detectors for varying amounts of analyte. The underlying experiments are described in Sect. 3 and their results are discussed in Sect. 4. Section 5 summarises the results of this work.

2 Instrumental

An overview of the analytical system used in this work is displayed in Fig. 1. Explanations regarding the individual components are given in the following subsections.

2.1 Preconcentration unit

Atmospheric mixing ratios (mole fraction) of halocarbons are very low, i.e. in the parts per trillion (ppt) to parts per quadrillion range (ppq). To achieve signals clearly distinguished from noise in GC MS analysis, a sample preconcentration procedure is required. In this work, the method of sample cryofocusation on adsorptive material followed by thermodesorption prior to gas chromatographic separation was used. Figure 2 shows a schematic of the preconcentration unit; explanations are given in the following. A similar setup was described by (Sala et al., 2014). A 1/16 inch stainless

AMTD
7, 12323–12355, 2014

steel tube (sample loop) packed with HayeSep D adsorption material was cooled to a temperature of −80 °C for cryofocusation. For cooling, a Stirling cooler was used (Global Cooling, Inc., model M150). The sample loop was was placed inside a cooled aluminium cylinder (cooling head) and was thermally and electrically isolated with two layers of glass silk and one layer of Teflon shrinking hose. The cooling head was thermally isolated towards ambient air with two layers of Aeroflex-HF material. All sample components which were not trapped on the adsorption material were collected in a 2 L stainless steel flask equipped with a pressure sensor (P) (see Fig. 1). The pressure difference between beginning and end of the preconcentration phase was recorded to calculate the preconcentration volume. After the preconcentration phase, the sample loop was heated resistively to +172 °C in a few seconds for instantaneous injection of the trapped analyte fraction onto the GC column. Desorption temperature was maintained for 4 min to clean the sample loop from all remaining compounds. All tubing (stainless steel) used for sample transfer between sample flask and preconcentration unit as well as preconcentration unit and GC was heated to 80 °C to avoid loss of analytes to the tubing wall.

2.2 Gas chromatograph

An Agilent Technologies 7890A GC with a Gas Pro PLOT column (0.32 mm inner diameter) was used for separation of analytes according to their boiling points. The column had a total length of 30 m, divided inside the GC oven into 7.5 m pre-column (backwards flush-able) and 22.5 m main-column. Purified Helium 5.0 (Alphagaz 1, Air Liquide, Inc.) was used as carrier gas. The GC was operated with constant carrier gas pressure on both pre- and main column. The temperature program of the GC consisted of five phases. (1) For the first two minutes, the temperature was kept at 50 °C. (2) Then the oven was heated with a rate of 15 °C minute^{-1} up to 95 °C, (3) from thereon 10 °C minute^{-1} up to 135 °C and (4) with a rate of 22 °C minute^{-1} up to 200 °C. (5) The final temperature of 200 °C was kept for 2.95 min. The resulting runtime was 17.95 min. The pre-column was flushed backwards with carrier gas after 12.6 min to avoid contam-

AMTD
7, 12323–12355, 2014

ination with high-boiling substances. The gas chromatographic column was connected to the QP MS and the TOF MS using a Valco three port union and two fused silica transfer lines. The split ratio of the gas flow after the GC was ≈ 34 % into the QP MS and ≈ 66 % into the TOF MS. The transfer line to the QP MS had a total length of 0.60 m with an inner diameter of 0.1 mm, the transfer line to the TOF MS had a total length of 2.54 m with an inner diameter of 0.15 mm. All parts of the transfer lines outside the GC oven were heated to 200 °C.

2.3 Mass spectrometer

The two mass spectrometers in comparison were (1) an Agilent Technologies 5975C QP MS and (2) a Markes International (former ALMSCO) Bench TOF-dx E-24 MS. Both MS were operated in electron ionisation (EI) mode with an ionisation energy of 70 eV and ioniser temperatures of 230 °C. The QP MS was operated in SIM and SCAN mode (see Table 2 for more information). As the GC was operated in constant pressure mode, i. e. the head pressure of the columns were kept constant, the carrier gas flow into the two MS therefore varied according to the temperature ramp during each gas chromatographic run. Pressures inside the ion flight tubes of the MS therefore also varied; the TOF MS had a pressure range from 1.8×10^{-6} to 1.6×10^{-6} hPa and the QP MS had a pressure range from 2.1×10^{-5} to 1.8×10^{-5} hPa. The Bench TOF-dx uses a direct ion extraction technique with an acceleration voltage of 5 kV. In contrast to many other TOF instruments the ions are accelerated directly from the ion source into the drift tube, instead of extracting them from the ion source and then accelerating them orthogonally to the extraction direction (orthogonal extraction). The direct extraction method in combination with the high acceleration energy orients the instrument towards a high sensitivity, especially for heavier ions (five technologies GmbH, G. Horner and P. Schanen, personal communication, 2014). The MS was set up to detect mass ranges from 45 to 500 m/z; higher and lower m/z were discarded. The reason to discard ions with m/z ratio below 45 was to eliminate a large part of the CO_2 which is trapped by our preconcentration method and can lead to saturation of the detector. A schematic of

AMTD
7, 12323–12355, 2014

the Bench TOF-dx is given in Fig. 3. The spectra extraction rate was adjusted to 4 Hz to get a data acquisition rate comparable to that of the QP MS.

3 Experimental

All characterisation experiments were conducted using a high-pressure air sample (50 L Aluminium flask, 70 bar) filled in 2007 at Jungfraujoch, Switzerland. Prior to preconcentration, the air sample was dried using a heated (70 °C) $Mg(ClO_4)_2$ water trap. Halocarbon mixing ratios were assigned to this reference gas by calibration against an AGAGE (Advanced Global Atmospheric Gas Experiment) gas standard (H-218). Table 1 shows reference gas mixing ratios of specific substances discussed in this paper.

3.1 Measurement procedure

To ensure measurement quality, both MS were tuned in regularly intervals (autotune by operating software). Additionally, a zero measurement (evacuated sample loop), a blank measurement (preconcentration of purified Helium 5.0) and two calibration gas measurements were conducted to condition the system before every measurement series. At the end of every measurement series, another blank measurement was added. Every measurement series itself consisted of a calibration measurement followed by two sample measurements (same sample). This sequence of three measurements was repeated *n*-times depending on the type of experiment and then terminated by a calibration measurement. For characterisation experiments both calibration and sample measurements were taken from the same gas cylinder (reference gas, see description above) but treated differently in data evaluation, e.g. as a calibration- or sample measurement. The integrated detector signal was divided by the preconcentration volume to get the detector response per sample volume. To account for detector drift during measurement series, the calibration measurements bracketing the sample pairs were interpolated linearly. Thereby, interpolated calibration points are generated for each

AMTD
7, 12323–12355, 2014

sample measurement. The response for each sample was then derived by calculating the quotient between sample and corresponding interpolated calibration point. Experiments were conducted to analyse five key parameters (Sects. 3.2 to 3.6) important for measurements of halogenated trace gases in the atmosphere: mass resolution, mass accuracy, limits of detection, measurement precision and reproducibility as well as detector linearity.

3.2 Mass resolution

The mass resolution (R) is defined as follows:

$$R = \frac{m}{\Delta m} \tag{1}$$

with Δm being the Full Width at Half Maximum (FWHM) of the exact mass m of the ion signal in u.

The mass resolution determines if two neighbouring mass peaks can be separated from each other. It is considered an instrument property, i.e. influenced only by internal factors like instrument geometry, ion optics etc. The mass resolution of the TOF MS was calculated with its operating software ProtoTOF in a mass calibration tune. The QP MS was operated with MS Chemstation (Agilent Technologies, Inc.) which only processes unit mass resolution.

3.3 Mass accuracy

The Mass accuracy (δa) defined as:

$$\delta a\,[\text{ppm}] = \frac{m - m_\text{m}}{m_\text{m} \times 10^{-6}} \tag{2}$$

quantifies the deviation between a measured ion mass m_m and the according expected exact mass m of the according fragment. Like mass resolution, it is considered an in-

AMTD
7, 12323–12355, 2014

strument property. In this work, so called 1 amu centroid mass spectra are used to calculate mass accuracy. The exact mass hereby is taken as the maximum intensity of the mass spectrum within a certain window (±0.5 u) around the nominal mass. Mass accuracy was calculated for four different ion masses (68.995, 84.966, 100.936, 150.933 u) which cover most of the mass range of the substance peaks in our chromatogram. Individual values for the mass accuracy were taken at the maximum of the according chromatographic peak. Data from reproducibility experiments (see Sect. 3.5) as well as regular sample measurements were analysed to gain information about (1) mass accuracy over multiple chromatographic runs and (2) mean mass accuracy over multiple measurement series for four exemplary ion masses. Only measurements taken under well equilibrated conditions were used for this analysis to minimise matrix effects.

3.4 Limits of detection

The lowest amount of a substance that can reliably be proven is considered to be its limit of detection (LOD) and serves as a measure for the sensitivity of the analytical system. Based on the assumption that a molecule fragment f can be detected when its detector signal height H_{f_i} is equal to or higher than three times the signal noise N_{f_i} on the adjacent baseline (signal-to-noise level (S/N) > 3), a limit of detection (LOD) for a fragment f_i from an analyte substance S_i with a mass m_{S_i} in the injected sample can be calculated as:

$$\mathrm{LOD}_{S_i} = \frac{3 \cdot N_{f_i} \cdot m_{S_i}}{H_{f_i}} \quad (3)$$

For comparison with the QP MS, the LOD of both instruments were calculated from calibration gas measurements by linear down scaling. Possible detector non-linearities were omitted in this case. The LOD error was considered to be the standard deviation of 10 calculated Limits of Detection. Different settings of the QP MS (SCAN mode (1), optimised (opti.) SIM mode (2) and operational (oper.) SIM mode (3)) were applied.

AMTD
7, 12323–12355, 2014

In the SCAN mode (1), the Quadrupole MS scanned from 50 to 500 u (comparable to the mass range of the TOF MS) with a dwell time of ≈ 3.7 ms ion^{-1} and a scan rate of 1.66 scans per second. In the optimised SIM mode (2), the Quadrupole MS measured only one ion with a dwell time of 310 ms with ≈ 3 scans per second. In the operational SIM mode (3) the Quadrupole MS measured several masses (up to six) in one scan with individual dwell times given in Table 2 and ≈ 3 scans per second.

The LOD in pg and ppq were calculated for 0.28 L sample volume with respect to the split ratio (see Sect. 2.2) and then extrapolated to 1 L of ambient air.

3.5 Reproducibility and measurement precision

The measurement precision describes the repeatability of a measurement. We determine the precision from the reproducibility (i.e. the standard deviation) of the measurements. The mean reproducibility is derived from dedicated multiple experiments designed to assess measurement precision (reproducibility experiment). Reproducibility was analysed over five measurement series, conducted on five different days, to give the mean measurement precision. Every experiment followed the procedure described in Sect. 3.1, with a total of 19 evaluated measurements of the same ambient air sample. A subset of the samples was treated as standard, the other part as unknown samples (two samples bracketed by two standards. Every individual measurement of these five series was conducted with a preconcentration volume of 0.28 L of the reference gas. An additional reproducibility experiment was conducted with a higher preconcentration volume of 1 L to assess the possible dependence of the reproducibility on the preconcentrated sample volume. The bracketing calibration points were interpolated point to point giving a calculated calibration value for every sample. The quotient of sample and calculated calibration value gives the relative detector response for the respective sample. For each sample pair, a standard deviation of the relative response was calculated, summed up over all pairs and divided by the number of pairs to form the sample pair measurement reproducibility of that measurement series. The described procedure was applied to all analysed substances and five reproducibility experiments.

AMTD
7, 12323–12355, 2014

The mean value of all five measurement reproducibilities is considered to be the measurement precision of the system for the respective substance.

3.6 Detector linearity

Detector linearity was analysed in two linearity experiments by varying the default preconcentration volume of 0.28 L by factors of 0.33, 0.66, 1.25 and 2 (sample positions in the measurement sequence, see Sect. 3.1). As calibration measurements, the default preconcentration volume was used. For comparison, detector responses were calculated as the ratio of the area of a chromatographic peak (A) to the preconcentration volume (V). All detector responses were normalised to one (relative detector response) by dividing them by the mean A/V of the calibration measurements. An ideally linear detector would show a relative response of 1 for any preconcentration volume used. The errors for the linearity measurements were derived as the three fold standard deviation given from reproducibility experiments.

4 Results and discussion

4.1 Mass resolution

If mass resolution is sufficiently high, it is possible to separate mass peaks of equal unit mass but differing exact mass. This separation drastically enhances the possibility to identify specific molecule fragments and to reduce cross-sensitivity. For halocarbon analysis, it is interesting to separate halogenated molecule fragments with exact masses typically below unit mass from other fragments with exact masses typically at or slightly above unit mass (e.g. hydrocarbon fragments). It could then be possible to reduce background noise generated by interfering ion signals or even compensate coelution of non-target species from the GC column. For quantitative analysis the separation of adjacent mass signals implicates a possible loss of signal area if both mass peaks are not fully be separated. The imposed error, i. e. the peak area lost due to

AMTD
7, 12323–12355, 2014

separation should not decrease measurement precision and should therefore be lower than the targeted measurement precision, in our case 0.1 %.

For this purpose, the definition of a qualitative and a quantitative separating resolution R_{Sep} is introduced (see Fig. 4 for an illustration). Assuming a Gaussian peak shape (normal distribution) of the ion signal on the mass axis a separation of two neighbouring signals m_1 and m_2 (with $m_2 > m_1$) by 8σ (SD, 4σ per peak) is considered a quantitative separation (less than 0.01 % loss of peak area) while a separation by less than 8σ is considered to be only a qualitative separation. Further assuming that 1σ is approximately 1/2 FWHM (or 1/2 Δm respectively) and that Δm_1 is not significantly different from Δm_2, one can estimate R_{Sep} (at m_1 or m_2) for a known ($m_2 - m_1$) difference:

$$R_{sep} = \frac{m_1}{\Delta m_1} = \frac{m_1}{\frac{2\cdot(m_2-m_1)}{n_\sigma}} \quad (4)$$

For values of $n_\sigma \geq 8$, Eq. (4) would give the quantitative separating resolution, for values of $n_\sigma > 2$ a qualitative separating resolution. Table 3 shows some examples for qualitative and quantitative separating resolutions required for separation of halogenated mass fragments from hydrocarbon molecule fragments with slightly different masses.

To separate e.g. the $CClF_2^+$ ion signal from the $C_6H_{13}^+$ ion signal qualitatively, a resolution of 600 is necessary. For a quantitative separation, the mass resolution has to be $R = 3700$ according to the definition of 8σ separation (see above). For the Bench TOF-dx, the calculated mass resolution was $R = 1000$ at mass 218.985 u for the fragment C_4F_9 in a mass calibration tune by the software ProtoTOF. This allows a qualitative separation of two neighbouring mass peaks like the ones listed in Table 3, e.g. the separation of mass 84.966 u to mass 85.102 u. For a quantitative separation as defined above, the mass resolution of the Bench TOF-dx is not be sufficient without further data processing steps like a peak deconvolution.

AMTD
7, 12323–12355, 2014

4.2 Mass accuracy

While sufficient mass resolution is necessary for an unambiguous separation of two mass peaks, mass accuracy is in addition needed for chemical identification of the detected ion. The better the mass accuracy, the lower the number of possible fragments that might be the source of the mass signal. The mass accuracy for the Bench TOF-dx was found to be in a range of 50 to 100 ppm for a mass range from 69 to 151 u. At a mass resolution of R = 1000 at ion mass 85 u and an accuracy of 100 ppm, the mass difference between measured and exact mass would be 10 % of the FWHM of this mass peak (or 5 % at 50 ppm). The stability and absolute accuracy in the determination of the exact mass is thus not a significant additional limitation in the ability of the Bench TOF-dx to separate different ions (see Sect. 4.1). Further the mass accuracy is sufficient to unambiguously distinguish different ions as listed in Table 3.

4.3 Limits of detection

For halocarbon measurement, sensitivity is an important issue as atmospheric concentrations can be below 1 pg L^{-1} of ambient air, especially for newly released anthropogenic species. Table 4 shows the calculated LOD for the QP and the TOF MS for the four selected species with different measurement settings of the Quadrupole MS detector.

For the QP MS, the number of ions of a certain m/z ratio that reach the detector depend on the concentration and the dwell time. The dwell time represents the time interval in which the quadrupole mass filter is tuned to the specific mass-to-charge ratio (m/z) before switching to another. Lower dwell times will reduce respective signal intensity but allow for more different mass filter settings per scan, resulting in more different m/z monitored per time. Higher dwell times increase the detector sensitivity towards specified m/z ratios but reduce the number of m/z monitored per time. For this work, data based on three different instrument settings was used for LOD calculation (see Table 2). The SCAN mode of the QP MS was chosen for a direct comparison

AMTD
7, 12323–12355, 2014

with the TOF MS and is shown in Table 4 (1). The optimised SIM mode monitors only one m/z of the respective substance, Table 4 (2). In a normal measurement of ambient air, several m/z have to be monitored (operational SIM mode (3)) due to overlapping peaks and in order to measure a quantifier and a qualifier ion. The available dwell time thus has to be distributed amongst different m/z ratios. As a consequence, Limits of Detection are higher in such measurements as in the optimised SIM mode. Table 4 (3) shows the standard dwell times used for measurements for the four discussed substances and respective LOD.

In comparison to the QP MS, the TOF MS is up to 12 times more sensitive than the QP MS in the SCAN mode. In the optimised SIM mode with increased dwell times (2) for specific ion masses, Limits of Detection in Quadrupole MS and Time of Flight MS are similar. During routine measurements (operational SIM mode (3)), the Limits of Detection of the TOF MS were up to a factor of 3 lower than those of the QP MS.

4.4 Reproducibility

A high measurement precision is required as it is of great importance to detect very small variability of halocarbons in the atmosphere, e.g. to characterise trends of highly persistent substances (Montzka and Reimann, 2011; Montzka et al., 2009; Vollmer et al., 2006). Table 5 shows exemplary reproducibilities for both instruments based on a preconcentration volume of 0.28 L. The reproducibility is rather similar for both MS, with values below 1 % for the species with high ambient air concentrations and therefore high signal to noise levels (CFC-12 and CFC-11). For the species with lower concentration and lower signal to noise levels the reproducibility of the TOF seems to be slightly but not significantly better (see Table 5).

The measurement precisions shown in Table 5 are based on measurements with a relatively small sample volume. Larger preconcentration volumes should result in better reproducibilities as signal-to-noise levels are increased and error sources during sample preparation should become smaller relative to the sample volume. Therefore,

AMTD
7, 12323–12355, 2014

a reproducibility experiment with a lager preconcentration volume of 1 L was performed. The results are shown in Table 6.

The increase of the preconcentration volume to 1 L yields a significant improvement of the measurement precision. The high signal to noise species CFC-12 and CFC-11 now show reproducibilities below 0.3 % for the QP and for the TOF. For the low signal to noise species Halon-1211 and CH_3I the reproducibilities are improved by a factor of up to four for the TOF MS and by a factor of up to three for the QP MS, with the TOF instrument showing better reproducibilities. As for the TOF MS, the detector itself was found to be a limitation to higher preconcentration volumes as it showed saturation effects for some analysed ions already at 0.5 L preconcentrated sample. E.g. CFC-12 had to be evaluated on mass 87 u (relative abundance: 32.6 %) and CFC-11 on mass 103 u (relative abundance: 65.7 %) (NIST, 2014) as both main quantifier ion masses (85 and 101 u) showed saturation in the respective retention time windows. This is a specific problem of the Bench TOF dx used here due to the limited dynamic range of the Analogue to Digital converter.

4.5 Linearity

For the calculation of the mixing ratio of a measured substance, its detector signal has to be correlated with the signal of the same substance in a calibration measurement with known mixing ratio. If the detector behaves linearly, this correlation is linear and the calculation of the mixing ratio is straight forward. As mixing ratios in different air samples might vary to a great extent (e.g. diurnal variations of short-lived substances) (Sala et al., 2014; Derwent et al., 2012; Law and Sturges, 2011), a linear detector simplifies data evaluation to a great extent. Furthermore, retrospective analysis of substances that were not identified at the time of measurement is possible without an unknown error due to detector non-linearity. Figures 5 and 6 show linearity plots for the QP MS for the CFC-11 and CFC-12 based on two linearity experiments. The QP MS showed a linear behaviour within the measurement errors (3-fold measurement reproducibility for the respective substance). This linearity test includes possible effects of the pre-

AMTD
7, 12323–12355, 2014

concentration unit (quantitative adsorption and desorption) as well as the determination of the preconcentration volume, the GC and data processing (signal integration). Figures 5 and 6 illustrate exemplary results from the two linearity experiments for the TOF MS. For CFC-11 (Fig. 5) a deviation from linearity for small preconcentration volumes of nearly 10 % is observed, while detector behaviour is close to the ideal value for high preconcentration volumes. The red curve was derived based on the standard detector voltage of −2244.8 V. An decrease of the detector voltage by −30 V brought slight improvements but did not solve the issue. Figure 6 shows a linearity plot for the substance CFC-12. For CFC-12 the detector is considered to be linear within the error bars. Both detectors compared in this work depend on the same sample preparation and separation steps before detection. As measurement reproducibilities of QP MS and TOF MS were not significantly different, the direct comparison is possible without limitations. The examples displayed for the QP MS and the TOF MS are two of 35 substances measured and analysed. The QP MS showed linear behaviour for all substances within the uncertainty range. The TOF MS in contrast showed non-linear behaviour (like CFC-11) for two thirds of all 35 analysed species. Proportionality of detector signal against the amount of analyte in the sample over the given concentration range was thus found for the QP MS but only for some species in the TOF MS. If the detector does not behave linearly, the relationship between the integrated peak area and the atmospheric concentration has to be approximated by a fit function. In order to generate this fit function, additional measurements with varying preconcentration volumes are necessary before each measurement series. This procedure was found to be necessary for the TOF MS. It lengthens measurement series, implies an additional error source and requires additional time for data processing.

5 Conclusions

A Markes International Bench TOF-dx was compared to an Agilent Technologies 5975 QP MS with respect to the measurement of halogenated trace gases in the atmo-

AMTD
7, 12323–12355, 2014

sphere. Both detectors ran in parallel (1 : 2 split) after cryogenic preconcentration and gas chromatographic separation of the air sample. The comparison included the mass resolution, mass accuracy, the limit of detection (LOD), the measurement precision (reproducibility) and the detector linearity. The TOF MS showed a resolution of 1000 and a Δm of 0.071 at mass 219.995 u with a mass accuracy of 50 to 100 ppm. Therefore it is able to qualitatively separate ion signals at deferring exact mass but equal unit mass for example the mass 84.966 u from the mass 85.106 u by a Δm of 0.136. This qualitative mass separation of the TOF MS could be sufficient for improved substance identification and is an advantage over the QP MS. The QP MS does not allow for separation of exact masses as the mass resolution of QP MS instruments is generally too low ($R \approx 200$) for that purpose. The analysis of detection limits showed that the TOF MS is generally more sensitive than the QP MS (despite using selected ion monitoring mode). The LOD of the QP in the SCAN mode are up to a factor of 12 higher than the LOD of the TOF MS. LOD of the TOF MS are lower by factors of up to 3 (Table 4) in comparison to the QP MS with operational SIM mode settings used for routine measurements. In the SIM mode with only one quantifier (optimised SIM mode) the TOF MS is similar to the QP MS. In that respect, the TOF MS with its very high sensitivity and full mass range information provides a considerable advantage compared to a QP MS. The reproducibility of both instruments was found to be on an equal level with slightly better reproducibilities of the QP MS at high signal to noise levels and slightly better reproducibilities of the TOF MS for low-concentrated species. Regarding detector linearity, the Bench TOF-dx in its current configuration could not compete with the QP MS. A high degree of linearity is however necessary for high accuracy measurements in trace gas analysis. The encountered non-linearities necessitate a correction which adds an error source, especially if there is a large concentration difference between sample and calibration measurement. It furthermore complicates measurements as well as data evaluation. For other applications where concentration variability is significantly higher than the non-linearity of the detector, the observed detector non-linearities might not be of such high relevance. Concluding, the TOF MS does show advantages

AMTD
7, 12323–12355, 2014

in respect to mass resolution and sensitivity without losing the full mass spectra information. Persisting non-linearities are a big disadvantage but might be conquered in the future by developments in detector electronics. With reduced non-linearities, TOF MS could well be the technology of the future for the analysis of halogenated trace gases in the atmosphere. These conclusions are only valid for the Markes International TOF MS E-24 and atmospheric trace gas measurements and might turn out differently for another field of research or another TOF MS.

Acknowledgements. The authors would like to thank five technologies GmbH for the technical support of the Bench TOF-dx, Laurin Hermann for the mechanical design and construction of the cooling head. J. Hoker thanks the European Community's Seventh Framework Programme (FP7/2007–2013) in the InGOS project under grant agreement 284274 for financial support.

References

Brinckmann, S., Engel, A., Bönisch, H., Quack, B., and Atlas, E.: Short-lived brominated hydrocarbons – observations in the source regions and the tropical tropopause layer, Atmos. Chem. Phys., 12, 1213–1228, doi:10.5194/acp-12-1213-2012, 2012. 12326

Cohan, D. S., Sturrock, G. A., Biazar, A. P., and Fraser, P. J.: Atmospheric Methyl Iodide at Cape Grim, Tasmania, from AGAGE Observations, J. Atmos. Chem., 44, 131–150, doi:10.1023/a:1022481516151, 2003. 12344

Cooke, K. M., Simmonds, P. G., Nickless, G., and Makepeace, A. P. W.: Use of Capillary Gas Chromatography with Negative Ion-Chemical Ionization Mass Spectrometry for the Determination of Perfluorocarbon Tracers in the Atmosphere, Anal. Chem., 73, 4295–4300, doi:10.1021/ac001253d, 2001. 12325

Cunnold, D. M., Weiss, R. F., Prinn, R. G., Hartley, D., Simmonds, P. G., Fraser, P. J., Miller, B., Alyea, F. N., and Porter, L.: GAGE/AGAGE measurements indicating reductions in global emissions of CCl_3F and CCl_2F_2 in 1992–1994, J. Geophys. Res., 102, 1259–1269, doi:10.1029/96jd02973, 1997. 12344

Derwent, R. G., Simmonds, P. G., O´Doherty, S., Grant, A., Young, D., Cooke, M. C., Manning, A. J., Utembe, S. R., Jenkin, M. E., and Shallcross, D. E.: Seasonal cycles in short-

AMTD

7, 12323–12355, 2014

lived hydrocarbons in baseline air masses arriving at Mace Head, Ireland, Atmos. Environ., 62, 89–96, doi:10.1016/j.atmosenv.2012.08.023, 2012. 12337

Farman, J. C., Gardiner, B. G., and Shanklin, J. D.: Large losses of total ozone in Antarctica reveal seasonal ClO_x/NO_x interaction, Nature, 315, 207–210, doi:10.1038/315207a0, 1985. 12324

Hall, B. D., Engel, A., Mühle, J., Elkins, J. W., Artuso, F., Atlas, E., Aydin, M., Blake, D., Brunke, E.-G., Chiavarini, S., Fraser, P. J., Happell, J., Krummel, P. B., Levin, I., Loewenstein, M., Maione, M., Montzka, S. A., O'Doherty, S., Reimann, S., Rhoderick, G., Saltzman, E. S., Scheel, H. E., Steele, L. P., Vollmer, M. K., Weiss, R. F., Worthy, D., and Yokouchi, Y.: Results from the International Halocarbons in Air Comparison Experiment (IHALACE), Atmos. Meas. Tech., 7, 469–490, doi:10.5194/amt-7-469-2014, 2014. 12326

Ivy, D. J., Arnold, T., Harth, C. M., Steele, L. P., Mühle, J., Rigby, M., Salameh, P. K., Leist, M., Krummel, P. B., Fraser, P. J., Weiss, R. F., and Prinn, R. G.: Atmospheric histories and growth trends of C_4F_{10}, C_5F_{12}, C_6F_{14}, C_7F_{16} and C_8F_{18}, Atmos. Chem. Phys., 12, 4313–4325, doi:10.5194/acp-12-4313-2012, 2012. 12325

Jordan, A., Haidacher, S., Hanel, G., Hartungen, E., Märk, L., Seehauser, H., Schottkowsky, R., Sulzer, P., and Märk, T. D.: A high resolution and high sensitivity proton-transfer-reaction time-of-flight mass spectrometer (PTR-TOF-MS), Int. J. Mass Spectrom., 286, 122–128, doi:10.1016/j.ijms.2009.07.005, 2009. 12325

Kim, Y.-H. and Kim, K.-H.: Ultimate Detectability of Volatile Organic Compounds: How Much Further Can We Reduce Their Ambient Air Sample Volumes for Analysis?, Anal. Chem., 84, 8284–8293, doi:10.1021/ac301792x, 2012. 12325

Kundel, M., Huang, R.-J., Thorenz, U. R., Bosle, J., Mann, M. J. D., Ries, M., and Hoffmann, T.: Application of Time-of-Flight Aerosol Mass Spectrometry for the Online Measurement of Gaseous Molecular Iodine, Anal. Chem., 84, 1439–1445, doi:10.1021/ac202527a, 2012. 12325

Laube, J. C. and Engel, A.: First atmospheric observations of three chlorofluorocarbons, Atmos. Chem. Phys., 8, 5143–5149, doi:10.5194/acp-8-5143-2008, 2008. 12326

Laube, J. C., Hogan, C., Newland, M. J., Mani, F. S., Fraser, P. J., Brenninkmeijer, C. A. M., Martinerie, P., Oram, D. E., Röckmann, T., Schwander, J., Witrant, E., Mills, G. P., Reeves, C. E., and Sturges, W. T.: Distributions, long term trends and emissions of four perfluorocarbons in remote parts of the atmosphere and firn air, Atmos. Chem. Phys., 12, 4081–4090, doi:10.5194/acp-12-4081-2012, 2012. 12325

AMTD
7, 12323–12355, 2014

Laube, J. C., Newland, M. J., Hogan, C., Brenninkmeijer, C. A. M., Fraser, P. J., Martinerie, P., Oram, D. E., Reeves, C. E., Röckmann, T., Schwander, J., Witrant, E., and Sturges, W. T.: Newly detected ozone-depleting substances in the atmosphere, Nat. Geosci., 7, 266–269, doi:10.1038/ngeo2109, 2014. 12325

Law, K. S. and Sturges, W. T. L. A.: Global Ozone Research and Monitoring Report – Chapter 2, WMO, Geneva, Switzerland, 2011. 12337

Lee, J. M., Sturges, W. T., Penkett, S. A., Oram, D. E., Schmidt, U., Engel, A., and Bauer, R.: Observed stratospheric profiles and stratospheric lifetimes of HCFC-141b and HCFC-142b, Geophys. Res. Lett., 22, 1369–1372, doi:10.1029/95gl01313, 1995. 12325

Miller, B. R., Weiss, R. F., Salameh, P. K., Tanhua, T., Greally, B. R., Mühle, J., and Simmonds, P. G.: Medusa: A Sample Preconcentration and GC/MS Detector System for in Situ Measurements of Atmospheric Trace Halocarbons, Hydrocarbons, and Sulfur Compounds, Anal. Chem., 80, 1536–1545, doi:10.1021/ac702084k, pMID: 18232668, 2008. 12325

Molina, M. J. and Rowland, F. S.: Stratospheric sink for chlorofluoromethanes: chlorine atomc-atalysed destruction of ozone, Nature, 249, 810–812, doi:10.1038/249810a0, 1974. 12324

Montzka, S. A. and Reimann, S. L. A.: Global Ozone Research and Monitoring Report – Chapter 1, WMO, Geneva, Switzerland, 2011. 12324, 12336

Montzka, S. A., Hall, B. D., and Elkins, J. W.: Accelerated increases observed for hydrochlorofluorocarbons since 2004 in the global atmosphere, Geophys. Res. Lett., 36, L03804, doi:10.1029/2008gl036475, 2009. 12336

NIST: National Institute of Standards and Technology: Mass Spectral Search Program for the NIST/EPA/NIH Mass Spectral Library, Gaithersburg, MD, USA, 2014. 12337

Prinn, R. G., Weiss, R. F., Fraser, P. J., Simmonds, P. G., Cunnold, D. M., Alyea, F. N., O'Doherty, S., Salameh, P., Miller, B. R., Huang, J., Wang, R. H. J., Hartley, D. E., Harth, C., Steele, L. P., Sturrock, G., Midgley, P. M., and McCulloch, A.: A history of chemically and radiatively important gases in air deduced from ALE/GAGE/AGAGE, J. Geophys. Res., 105, 17751–17792, doi:10.1029/2000jd900141, 2000. 12344

Sala, S., Bönisch, H., Keber, T., Oram, D. E., Mills, G., and Engel, A.: Deriving an atmospheric budget of total organic bromine using airborne in situ measurements from the western Pacific area during SHIVA, Atmos. Chem. Phys., 14, 6903–6923, doi:10.5194/acp-14-6903-2014, 2014. 12325, 12326, 12337

Solomon, S.: Progress towards a quantitative understanding of Antarctic ozone depletion, Nature, 347, 347–354, doi:10.1038/347347a0, 1990. 12324

AMTD
7, 12323–12355, 2014

Vollmer, M. K., Reimann, S., Folini, D., Porter, L. W., and Steele, L. P.: First appearance and rapid growth of anthropogenic HFC-245fa ($CHF_2CH_2CF_3$) in the atmosphere, Geophys. Res. Lett., 33, L20806, doi:10.1029/2006GL026763, 2006. 12336

Vollmer, M. K., Miller, B. R., Rigby, M., Reimann, S., Mühle, J., Krummel, P. B., O'Doherty, S., Kim, J., Rhee, T. S., Weiss, R. F., Fraser, P. J., Simmonds, P. G., Salameh, P. K., Harth, C. M., Wang, R. H. J., Steele, L. P., Young, D., Lunder, C. R., Hermansen, O., Ivy, D., Arnold, T., Schmidbauer, N., Kim, K.-R., Greally, B. R., Hill, M., Leist, M., Wenger, A., and Prinn, R. G.: Atmospheric histories and global emissions of the anthropogenic hydrofluorocarbons HFC-365mfc, HFC-245fa, HFC-227ea, and HFC-236fa, J. Geophys. Res., 116, D08304, doi:10.1029/2010jd015309, 2011. 12325

AMTD
7, 12323–12355, 2014

Table 1. Mixing ratios in ppt in the reference gas used in this work for the discussed substances.

Substance	Formula	MR [ppt]	Scale
CFC-12	CCl_2F_2	544.42	SIO-05
CFC-11	CCl_3F	250.79	Prinn et al. (2000)
Halon 1211	$CBrClF_2$	4.41	Cunnold et al. (1997)
Iodomethane	CH_3I	0.88	NOAA-Dec09 Cohan et al. (2003)

AMTD
7, 12323–12355, 2014

Table 2. Dwell time settings for given substance fragments in QP MS modes with a data frequency of ≈ 3 Hz. SCAN mode (1): QP scanned from 50 to 500 u with 1.66 scans per second and a dwell time of 3.7 ms. Optimised (opti.) SIM mode (2): settings used for measurements that LOD calculation was based on with 310 ms dwell time per ion and a scan rate of 3 scans per second. Operational SIM mode (3): default settings, used for reproducibility and linearity experiments with 3 scans per second.

Substance	Fragment	m/z [u]	QP SCAN mode dwell time [ms] for LOD calculation (1)	optimised (opti.) SIM mode dwell time [ms] for LOD calculation (2)	operational (oper.) SIM mode dwell time [ms] for LOD calculation (3)
			1.66 scans per second	3 scans per second	3 scans per second
CFC-12	$CCl^{35}F_2^+$	85	50 to 500 u		50
CFC-11	$CCl_2^{35}F^+$	101		310 ms dwell time	70
Halon 1211	$CCl^{35}F_2^+$	85	3.7 ms dwell time		100
Iodomethane	CH_3I^+	142			70

AMTD
7, 12323–12355, 2014

Table 3. Three exemplary halocarbon/hydrocarbon fragment pairs with equal unit mass but differing exact mass. The qualitative separating resolution (qual. R_{sep}) with $n_\sigma = 2$ and the quantitative separating resolution (quan. R_{sep}) with $n_\sigma = 8$.

Fragment	Exact mass m [u]	Δm [u]	qual. R_{sep} ($n_\sigma = 2$)	quant. R_{sep} ($n_\sigma = 8$)
$CClF_2^+$	84.966	0.136	> 600	> 2500
$C_6H_{13}^+$	85.102			
CF_3^+	68.995	0.075	> 900	> 3700
$C_5H_9^+$	69.070			
$C_2H_3Cl_2^+$	98.958	0.159	> 600	> 2500
$C_7H_{15}^+$	99.117			

AMTD
7, 12323–12355, 2014

Table 4. The limit of detection (LOD) in ppq and pg of the substances CFC-12, CFC-11, Halon-1211 and Iodomethane in 1 L of air sample per detector. The used dwell times and settings for the QP MS are given in Table 2.

Substance	LOD TOF [ppq]	LOD TOF [pg]	LOD QP [ppq] SCAN (1)	LOD QP [pg] SCAN (1)	LOD QP [ppq] opti. SIM (2)	LOD QP [pg] opti. SIM (2)	LOD QP [ppq] oper. SIM (3)	LOD QP [pg] oper. SIM (3)
CFC-12	25 ± 2	0.12 ± 0.02	241 ± 19	1.18 ± 0.09	21 ± 3	0.10 ± 0.01	48 ± 6	0.23 ± 0.30
CFC-11	31 ± 2	0.17 ± 0.02	370 ± 19	2.05 ± 0.29	36 ± 1	0.20 ± 0.01	64 ± 9	0.35 ± 0.05
Halon-1211	27 ± 2	0.182 ± 0.004	276 ± 53	1.84 ± 0.13	36.0 ± 0.3	0.240 ± 0.002	43 ± 5	0.29 ± 0.02
Iodomethane	12.00 ± 0.01	0.069 ± 0.001	Not a Number	Not a Number	16 ± 1	0.090 ± 0.003	42 ± 2	0.24 ± 0.05

AMTD
7, 12323–12355, 2014

Table 5. The reproducibility (REP) for the QP MS and the TOF MS as a mean value of five measurement series with 20 measurements each and a preconcentration volume of 0.28 L.

Substance	Formula	REP QP [%]	REP TOF [%]
CFC-12	CCl_2F_2	0.56 ± 0.31	0.56 ± 0.18
CFC-11	CCl_3F	0.45 ± 0.26	0.54 ± 0.23
Halon-1211	$CBrClF_2$	1.56 ± 0.52	0.94 ± 0.39
Iodomethane	CH_3I	3.96 ± 0.72	3.44 ± 1.61

AMTD
7, 12323–12355, 2014

Table 6. Measurement Precision (MP) for the QP MS and the TOF MS based on a single reproducibility experiment with a preconcentration volume of 1.0 L.

Substance	Formula	MP QP [%]	MP TOF [%]
CFC-12	CCl_2F_2	0.27	0.29
CFC-11	CCl_3F	0.12	0.16
Halon-1211	$CBrClF_2$	0.56	0.40
Iodomethane	CH_3I	1.14	0.78

AMTD
7, 12323–12355, 2014

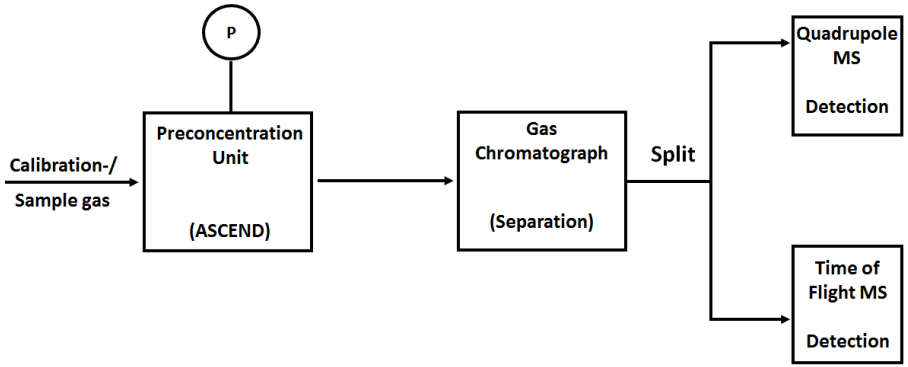

Figure 1. Schematic of the analytical setup, All sample components which cannot be cryofocused are collected in a stainless steel flask equipped with a pressure sensor (*P*) for sample volume determination. After preconcentration, the sample is thermally desorbed and transported into the GC via the carrier gas flow. After gas chromatography, the flow is splitted by a 3-way-split inside the GC oven into the Quadrupole MS and in the Time of Flight MS for detection of the analytes.

AMTD
7, 12323–12355, 2014

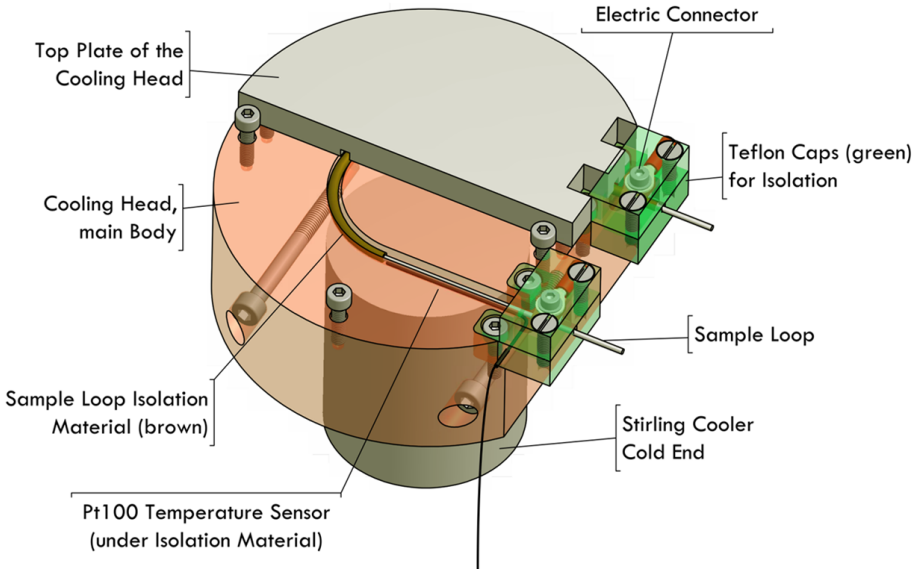

Figure 2. Schematic of the cooling head. The aluminium cylinder which contains the sample loop is placed on top of the Stirling coolers' cold end. Electric connectors are located at each end of the sample loop for resistive heating.

AMTD
7, 12323–12355, 2014

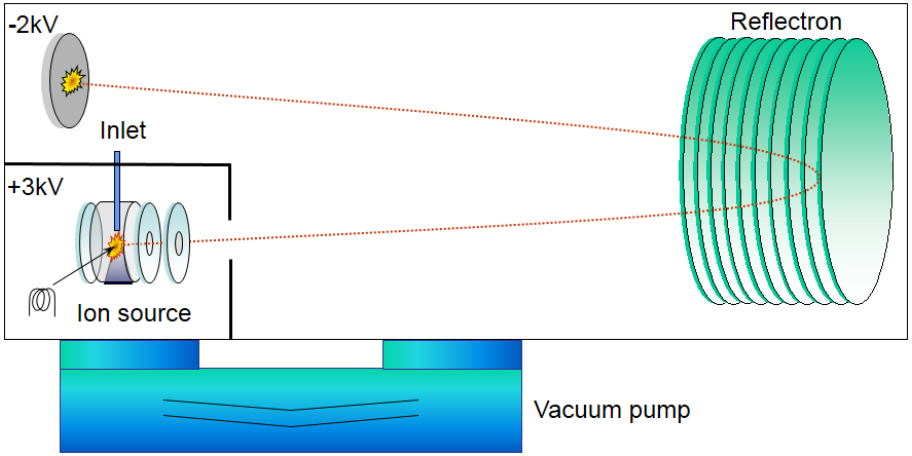

Figure 3. Scheme for the direct ion extraction of the Bench TOF dx direct extraction (five technologies GmbH, G. Horner and P. Schanen, personal communication, 2014). The red dotted line represents a typical ion path.

AMTD
7, 12323–12355, 2014

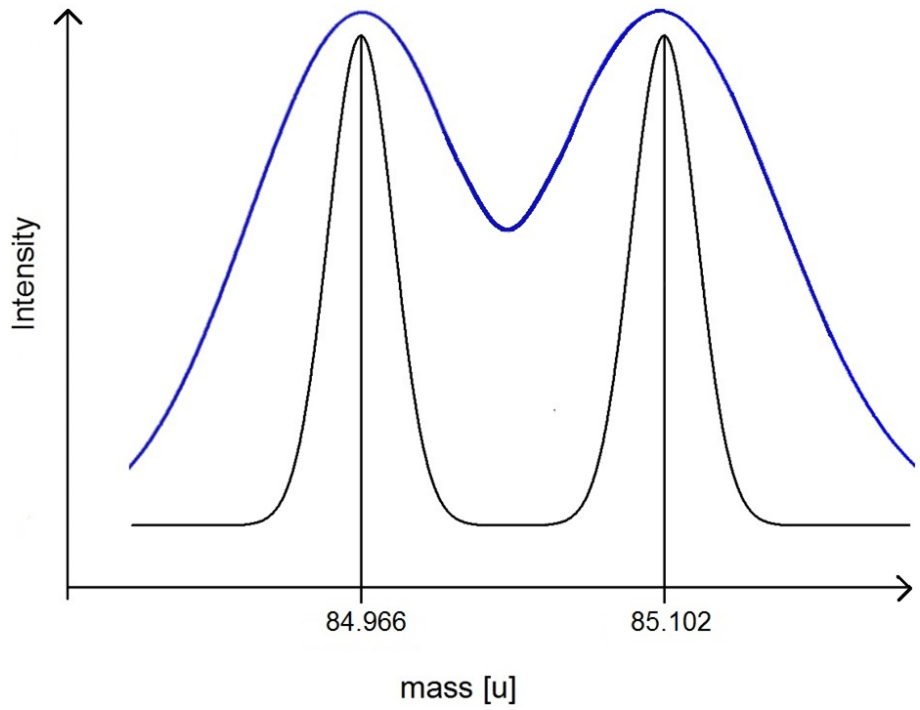

Figure 4. Schematic display of two different mass resolutions (blue and black curve). Two signals on masses 84.966 and 85.102 u with equal intensities demonstrate the mass separation with R = 600 (blue curve) and R = 3700 (black curve). Assuming Gaussian peak shapes for the signals, R = 3700 separates both peak by 8σ (quantitative separation), R = 600 separates them by only 2σ (qualitative separation).

AMTD
7, 12323–12355, 2014

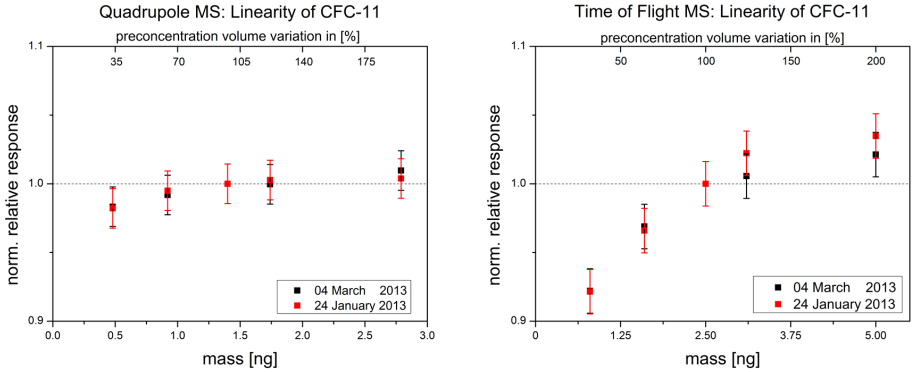

Figure 5. Linearity graphs of CFC-11 ($CFCl_2^+$ fragment), based on two different linearity experiments (red and black plots in each graph). Primary *x* axis (lower): mass on column in ng. Secondary *x* axis (upper): preconcentration volume variation in % vs. a default preconcentration volume of 0.3 L. *y* axis: relative detector response (vs. the detector response of the default preconcentration volume). For every preconcentration volume, the relative response should be one in case of a linear detector behaviour (dashed line). The errorbars show the three fold measurement precision. On the left hand side for the QP MS and on the right hand side for the TOF MS. The second linearity experiment (black) of the TOF MS was conducted with an decreased detector voltage (−2274.8 V instead of −2244.8 V).

AMTD
7, 12323–12355, 2014

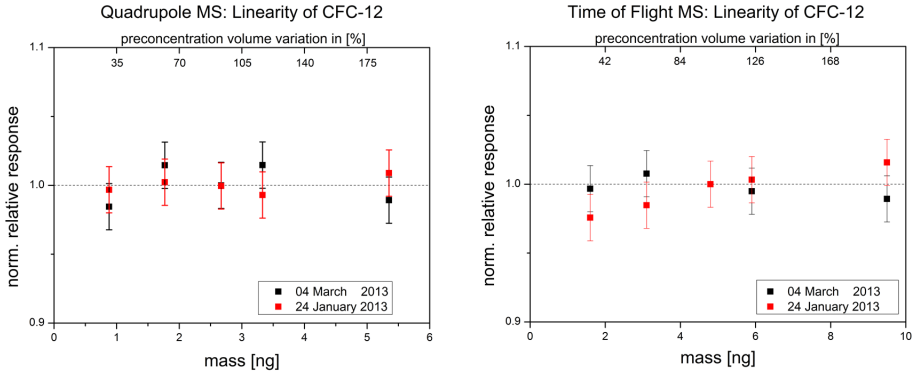

Figure 6. Same figure as Fig. 5 for the substance CFC-12 (CF_2Cl^+ fragment).

AMTD
7, 12323–12355, 2014

Application of GC/Time-of-Flight-MS for halocarbon trace gas analysis

J. Hoker et al.